

$\bar{N}N$ INTERACTION THEORETICAL MODELS

B. LOISEAU

Division de Physique Théorique*, Institut de Physique Nucléaire, 91406 Orsay
Cedex, France and LPTPE, Université P. et M. Curie, 4 Place Jussieu 75252
Paris Cedex 05, France

Invited talk to the 13th International Conference on Few Body Problems in
Physics, Adelaide, Australia, January 5-11, 1992, to be published in the
proceedings (special issue of Nuclear Physics A).

IPNO/TH 91-97

DECEMBER 1991

* Unité de Recherche des Universités Paris 11 et Paris 6 Associée au CNRS.

$\bar{N}N$ interaction theoretical models

B. loiseau

Division de Physique Théorique*, Institut de Physique Nucléaire, 91406 Orsay Cedex, France and LPTPE, Université P. et M. Curie, 4 Place Jussieu 75252 Paris Cedex 05, France

Abstract

In this talk on Antinucleon-nucleon ($\bar{N}N$) interaction theoretical models we shall try to show which is our present understanding on the $\bar{N}N$ interaction, either from quark- or/and meson- and baryon-degrees of freedom, by considering the $\bar{N}N$ annihilation into mesons and the $\bar{N}N$ elastic and charge-exchange scattering.

1. INTRODUCTION

There has been, in the last eight years or so, a renewal of interest for the study of the $\bar{N}N$ interaction at low and medium energy due to new experimental results with low-energy antiproton beams, mainly at 1) Brookhaven National Laboratory (BNL, USA), 2) the National Laboratory of High Energy Physics (KEK, Japan) and 3) LEAR (Low Energy Antiproton Ring, CERN) (see e.g. ref. 1 to 5). Furthermore, since 1988, with a much improved beam at LEAR, more elaborate experiments have been, are being or will be performed.

The $\bar{N}N$ interaction is very different from the better known and studied NN interaction. The $\bar{N}N$ system, characterised by a baryon number zero annihilates easily into mesons. It is, right from threshold, a multichannel process. One difficulty will be to build up a model which explains in a consistent way both the elastic scattering data and the annihilation.

On the other hand the experimental and theoretical developments of the last 25 years have given us a relatively good understanding of the structure of the nucleon. In a qualitative way one picture of the nucleon can be depicted as a core composed of three valence quarks (q), plus gluons (g), plus sea quarks (antiquark (\bar{q})-quark pairs), surrounded by a cloud of mesons, pions (π), plus vector mesons ρ , ω ... The radius r_c of the core is thought to be of the order of .5 fm. The extension in space of the nucleon is of the order of 2 fm. This picture leads us to see that the degrees of freedom needed to describe the $\bar{N}N$ interaction will be twofold : at long range the meson degrees of freedom

* Unité de Recherche des Universités Paris 11 et Paris 6 Associée au CNRS.

are expected to play the main role and at short range the quark-gluon degrees of freedom should be more adequate to describe the phenomena.

In this review on $\bar{N}N$ interaction theoretical models we shall try to show which is our present understanding on the $\bar{N}N$ interaction at low and medium energy either from quark-or/and meson-and baryon-degrees of freedom. We shall do it by reporting on some recent theoretical works : - on the $\bar{N}N$ annihilation into mesons in section 2, and - on the $\bar{N}N$ elastic and charge-exchange scattering in section 3. Some outlook, discussion and conclusions will be given in section 4. This talk will not be a complete review on the subject and the interested reader will find more materials on the recent review article of ref. 1) and in the proceedings of the latest conferences or workshops devoted to the $\bar{N}N$ problem²⁻⁵).

2. $\bar{N}N$ ANNIHILATION INTO MESONS

In the physics of $\bar{N}N$ interaction the annihilation problem is the most complicated and may be the most interesting. Attempts to build up a theory for the annihilation from what we believe to be the theory of strong interaction, i.e. the quantum chromodynamic (QCD), have not been successful so far. The main reason is that the annihilation, taking place when the quark- and antiquark-cores overlap, has a characteristic size of the order of .6 to 1 fm. For such distances QCD is in a non-perturbative regime. Consequently the experimental results are analyzed in terms of various models. The study of the annihilation into mesons provides informations on the annihilation mechanism.

At low energy, antiproton annihilates a proton into a primary meson channel of a few mesons decaying into multiple final state. The average pion multiplicity is about 5 pions per annihilation with 1.8 π^0 . From the pion invariant mass distribution, in the final state, one observes production rates of primary two-three-or more-meson channels. For instance, the final state $2\pi^+2\pi^-\pi^0$ has the $\rho^0\omega$ state as a primary channel. The dominant annihilation consists of two-and three- body modes in the final state. One expects the two-meson final state to give the main contribution (at medium energy) in the in flight annihilation. At rest the three-meson contribution might dominate⁶). Different microscopic models either from quarks or hadronic diagrams have been considered. We shall report here on some recent aspects.

2.1 $\bar{N}N$ annihilation from quark-degrees of freedom

The quark dynamics is usually explained by studying the five basic quark line diagrams (QLD) of fig. 1. Many other diagrams can be generated from them by adding gluon lines in an arbitrary way. Which are their relative contributions to the annihilation cross section ? Which is the effective operator for a q - \bar{q} pair annihilation and creation ? The most popular q - \bar{q} annihilation and creation vertices are the scalar (3P_0 vertex) and the vector (3S_1 vertex) interactions. Before summarizing the status of the different recent models, let us review the discussion of ref. 7) (hereafter denoted by GMT) of the hierarchy of the different diagrams of fig. 1, investigations based only on the quark flavor flux within the QLD.

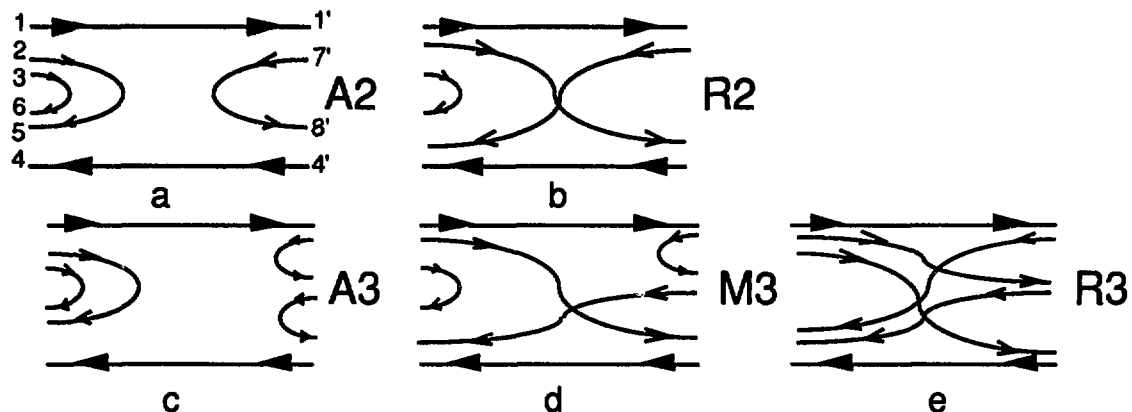


Figure 1. Different types of quark diagrams of $N\bar{N}$ annihilation into mesons characterized by different numbers of $q\bar{q}$ pair annihilations and creations and rearrangement of q or \bar{q} lines.

As recalled by GMT the validity of the quark line rule (QLR)⁸⁾ is based on the fact that a $s\bar{s}$ state can only be produced in $N\bar{N}$ annihilation together with strange particle. It is therefore important to find experimentally if there is a suppression of production of $s\bar{s}$ final states without associated strange particle production. The QLR can be tested by studying the $p\bar{p}$ annihilation into η and η' together with production of non-strange $M_1, M_2 \dots M_m$ pseudoscalar or vector mesons.

Let us illustrate some results of GMT by writing

$$\eta = x [u\bar{u} + d\bar{d}]/\sqrt{2} + y [s\bar{s}] + \text{gluon contribution} \quad (1)$$

$$\eta' = -y [u\bar{u} + d\bar{d}]/\sqrt{2} + x [s\bar{s}] + \text{gluon contribution}$$

If there is no gluon contribution, $x^2 + y^2 = 1$ and x^2 can be related to the pseudoscalar mixing angle, ϕ_{PS} by

$$x^2 = \sin^2(35.3^\circ - \phi_{PS}) \quad (2)$$

Validity of QLR gives relations between annihilation amplitudes T , for example, if production of η and η' together with non strange mesons comes mainly from their $u\bar{u} + d\bar{d}$ content then

$$yT(\eta, M_1, \dots, M_m) + xT(\eta', M_1, \dots, M_m) = 0 \quad (3)$$

GMT find that with the present data any $-26^\circ < \phi_{PS} < -2.2^\circ$ is approximately consistent with the QLR. They further study the consequence of eventual dominance of annihilation (figs. 1a and 1c) over rearrangement (figs. 1b and 1e) or mixed diagram (fig. 1d). They obtain relations between physical amplitudes via mixing as each quark line represents the same quark flavor everywhere in each diagram. For instance, dominance of annihilation (fig. 1a) predicts for the cross sections $\sigma(\omega\omega) = \sigma(\rho^0\rho^0)$. This relation is naturally verified

by the model A2 of ref. 16), see table 2, section 2.2). Experimental branching ratios are⁹⁾ $B(\rho^0\rho^0) = (0.12 \pm .12)\%$, $(.4 \pm .3)\%$, $B(\omega\omega) = (1.4 \pm 0.6)\%$ and $B(\rho^0\omega) = (2.26 \pm 0.23)\%$, $(0.7 \pm .3)\%$, $(3.49 \pm .59)\%$. This shows that, $\sigma(\omega\omega) = \sigma(\rho^0\rho^0)$, is satisfied within 2 error bars by the data. Dominance of rearrangement (fig. 1b) with $B(\rho^0\rho^0) = 0$ (from data), predicts $B(\omega\omega) = 2B(\rho^0\omega)$ which agrees only with one of the three sets of the above data. Other consequences of dominance of rearrangement or annihilation diagrams for $p\bar{p} \rightarrow 3$ mesons are also worked out. For instance dominance of rearrangement (fig. 1e) implies $x^4\sigma(\rho^0\pi^0\pi^0) = \sigma(\omega\eta\eta)$ and that of annihilation (fig. 1c) $x^4\sigma(\pi^0\pi^0\rho^0) = \sigma(\eta\eta\rho^0)$. However, further and more accurate experimental data are needed before concluding on the annihilation dominance model. Extension of the QLD, with flavor SU(3) symmetry, can give more relations between annihilation amplitudes¹⁰⁾. Possible violations of QLR have been recently discussed in ref. 11).

In more specific models^{1,6)} the 3P_0 vertex (fig. 2a) represents a q-qbar pair annihilation into gluon states with the quantum numbers of the vacuum while

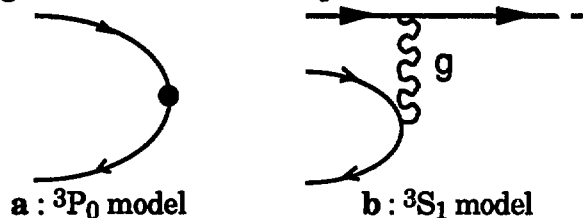


Figure 2. Two specific types of popular vertices for q-qbar annihilation

the 3S_1 (fig. 2b) corresponds to a q-qbar pair conversion into one gluon, then absorbed by another quark or antiquark. The 3S_1 model originates from perturbative QCD and is difficult to justify at the low momenta (~ 500 MeV/c) considered here. The present consensus favors the 3P_0 vertex as i) it is a model successful in describing the decay of mesons and baryons¹²⁾ ii) it can be derived from lattice QCD in the strong coupling limit¹³⁾. Let us mention a recent attempt¹⁴⁾ to estimate, in the flux-tube model, based on the strong coupling lattice QCD theory, the amplitude of a flux-tube breaking into two flux tubes and into three flux tubes. The strength of the flux-tube breaking is also compared to the empirical strength of the 3P_0 model. See also ref. 15) for earlier considerations on the flux tube mechanism in the $N\bar{p} \rightarrow N$ annihilation.

In a non-relativistic approach the transition amplitude of $p\bar{p}$ annihilation into two mesons M_1, M_2 can be written as^{6,16)} (see fig. 1a)

$$T_{A2} = \int d^3q'_1 d^3q'_7 d^3q'_8 d^3q'_4 d^3q_1 \dots d^3q_6 \psi_{M_1 M_2}^+ O_{A2} \psi_{N\bar{N}} \quad (4)$$

where $\psi_{M_1 M_2}$ and $\psi_{N\bar{N}}$ are the two-meson and the $N\bar{N}$ wave functions, usually described by a Gaussian for the internal quark motions. For example the spatial part of a S-wave meson, cluster of a q-qbar pair, will be

$$\phi_{M_1 M_2}(q_1' q_7') = N_s \exp[-b^2(q_1' - q_7')^2/8] \quad (5)$$

In these Gaussians the size parameters, b , of the baryons and mesons are usually chosen in such a way that $[\langle r_N^2 \rangle]^{1/2} \sim .6$ fm and $[\langle r_M^2 \rangle]^{1/2} \sim .5$ fm. The operator O_{A2} for the $2 q\bar{q}$ pair annihilation followed by a $q\bar{q}$ pair creation with a 3P_0 vertex in the QLD A2 (fig. 1a) is chosen as

$$O_{A2} = \lambda_{A2} \delta^3(\vec{q}_1 - \vec{q}'_1) \delta^3(\vec{q}_4 - \vec{q}'_4) V^{25} V^{36} (V^{7'8'})^+ \quad (6)$$

$$\text{with } V^{ij} = - \sum_{\alpha} \langle 1\alpha 1-\alpha | 00 \rangle \sigma_{-\alpha}^{ij} \left| \vec{q}_i - \vec{q}_j \right| Y_{1\alpha}(\vec{q}_i - \vec{q}_j) \delta^3(\vec{q}_i + \vec{q}_j) \quad (7)$$

The constant λ_{A2} , describing the effective strength of the annihilation process is a parameter to be fitted to the data. Similar transition amplitudes can be written for the different diagrams of fig. 1.

An overall reasonable fit of the branching ratios at rest and in flight indicates^{6,16,17}) that the annihilation model A2 + A3 (fig. 1a and 1c) with 3P_0 vertices for the q - q bar pair annihilation and creation plays an important role in the description of the low-energy annihilation mechanism of the $N\bar{N}$ system. However effects of initial and eventually final state¹⁵) (see sect. 2.2) interactions should be considered, they can be important^{6,18}). Relativistic effects¹⁹) have been studied, they were shown to be not too important leading in particular to an increase of the production of the light-meson channels.

2.2 $\bar{N}N$ annihilation from meson - and baryon-degrees of freedom

In a conventional meson-theoretical approach $N\bar{N}$ annihilation into two mesons can proceed via the exchange of baryons, N, Δ, \dots as shown in fig. 3. This is a short range process, its Compton wavelength being less than .2 fm ($\sim (\text{nucleon mass})^{-1}$). At such distance the hadronic picture might be ruled out. This range argument is however valid only for point like particle. Nevertheless

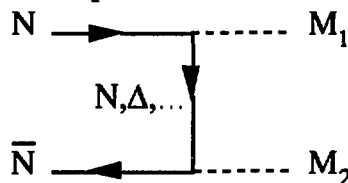


Figure 3. Baryon-exchange diagram of $N\bar{N}$ annihilation into two mesons

annihilation into two mesons with baryon exchanges can be calculated in a relatively straightforward way and could be thought as complementary to the quark-gluon dynamic approach reviewed in the previous section as it might show which are the limits of the hadronic model. An early work²⁰), using a distorted wave Born approximation (DWBA) with a semiphenomenological potential explained the gross features of some $p\bar{p}$ annihilation into 2 mesons. We shall briefly describe here the systematic study, recently performed in ref. 21), within the same line, and hereafter referred as MH3.

The annihilation amplitudes in MH3 are given by

$$\langle M_1 M_j | T | \bar{N}N \rangle = \langle M_1 M_j | V | \bar{N}N \rangle + \langle M_1 M_j | V | \bar{N}N \rangle G_0(\bar{N}N) \langle \bar{N}N | T | \bar{N}N \rangle \quad (8)$$

which is illustrated in fig. 4. Note that the transition potentials arise only

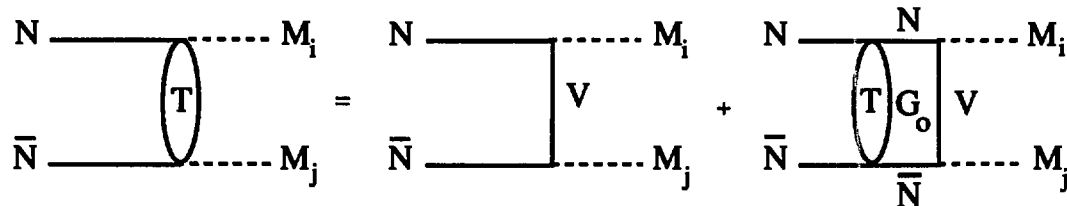


Figure 4. Pictorial representation of the DWBA approach.

from Nbar-N pair. The different mesons considered together with all annihilation transition potentials are depicted in fig.5. Most of the meson coupling constants

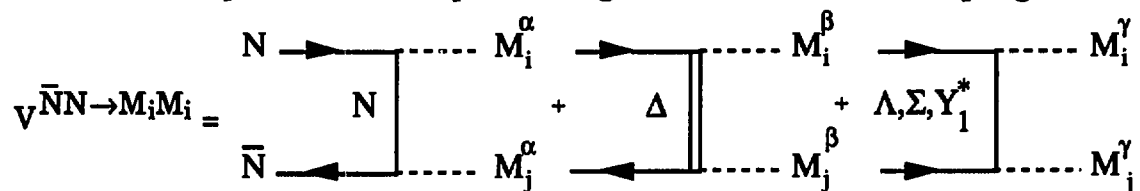


Figure 5. The different transition annihilation potentials used in ref. 21),

$$M_{ij}^{\alpha} = \pi, \eta, \eta', \rho, \omega, \delta, a_1, a_2, f_2, M_{ij}^{\beta} = \pi, \rho \quad \text{and} \quad M_{ij}^{\gamma} = K, K^* .$$

tants are taken from the Bonn NN model²²⁾ and its extension to the hyperon-nucleon case²³⁾. The cutoff masses of the form factors, needed to regularise the large momenta, are roughly adjusted by a fit on the available experimental branching ratio of the protonium annihilation at rest. Let us recall that the branching ratio, B_{ij} , is defined by the ratio of the partial width for the decay into meson i and j to the total annihilation width,

$$B_{ij} = \Gamma_{ij} / \Gamma_{\text{tot}} \quad (9)$$

$$\text{Here } \Gamma_{ij} = 2\pi k E \int d\Omega_{\mathbf{k}} | \langle k M_i M_j | V | \psi_{\text{NN}}^- \rangle |^2 \quad (10)$$

where E is the total c.m. energy. Γ_{tot} is obtained as the sum of all partial widths. As can be seen from eqs. (8) and (10) the knowledge of the initial state interaction is needed and in order to study its effects MH3 used 3 models²⁴⁾: A(BOX), A(OBE) and C, main characteristics of which are summarized in table 1. Some results are illustrated in table 2 where all B_{ij} of MH3 are calculated with the form factors for the transition potentials fitted with the model A(BOX) for the initial state. They are compared with the experimental data, with the A2 quark model¹⁶⁾ (see section 2.1) and the hadronic model of ref. 25^{a)}. There can be large discrepancies between the results obtained with different initial state interactions A and C although these models reproduce, with roughly the same quality, the Nbar-N data²⁴⁾ (see also section 3.1). If one uses the Born approximation only, the B_{ij} exceed the unitary limit²⁰⁾. Trend of the low momenta pbar-p annihilation in flight is roughly reproduced by the MH3 calculation. So far no final state interaction was considered, these could

Initial State $\bar{N}N$ interaction	Elastic part : G-parity on	Annihilation part (r in fm)
A(BOX)	Slightly modified full NN Bonn ²²⁾	$(-629-i 4567)e^{-r^2/2(.36)^2}$ MeV
A(OBE)	Simpler NN One Boson Exchange ²²⁾	$(-1260-i 1575)e^{-r^2/2(.4)^2}$ MeV
C	Slightly modified full NN Bonn ²²⁾	2 nd iteration of $\langle M_i M_j V \bar{N}N \rangle$

Table 1. Main characteristics of the initial state $\bar{N}N$ interaction used by MH3²¹⁾.

be important in particular for the $p\bar{p} \rightarrow \pi^+\pi^-$ annihilation as shown recently in ref. 26). This is illustrated in fig. 6 where some results are compared to the experimental data²⁷⁾ and to the model of ref. 20). The large

Channel $\bar{p}p \rightarrow$	A(BOX)	A(OBE) ref. 21	C	A2 ref. 16	HM ref. 25	Exp(%) ref. 9b
$\pi^+\pi^-$.39	.43	.21	.12	.34	$.33 \pm 0.017$
$\rho^\pm\pi^\mp$	1.09	.89	.575	2.1	2.82	1.7 ± 0.1
$\rho^0\pi^0$	0.58	.50	.43		.32	1.4 ± 0.1
$\rho^+\rho^-$	7.41	5.24	1.44			< 9.5
$\rho^0\rho^0$	1.07	.91	.077	0.4	.51	0.4 ± 0.3
$\rho^0\omega$	2.77	1.99	4.81	2.3	2.8	3.9 ± 0.6
$\omega\omega$	1.66	1.29	0.39	0.4	2.28	1.4 ± 0.6
K^+K^-	0.21	.13	.028		.03	0.1 ± 0.01

Table 2. Comparison of $B_{ij}(\%)$ of S-wave $p\bar{p}$ annihilation at rest.

difference, in the backward direction, in $d\sigma/d\Omega$ between models of refs. 21, 26) and that of ref. 20b) comes from a different choice of the Δ propagator. As advocated in ref. 28) the $\Delta(1236)$ degrees of freedom should be introduced and one should consider, in the hadronic picture, the process $N-N\bar{p} \rightarrow N-\Delta\bar{p}$ ($\Delta-\Delta\bar{p}$) pairs in the transition potentials (see fig. 4). One way to introduce the Δ will be the use of coupled channels.

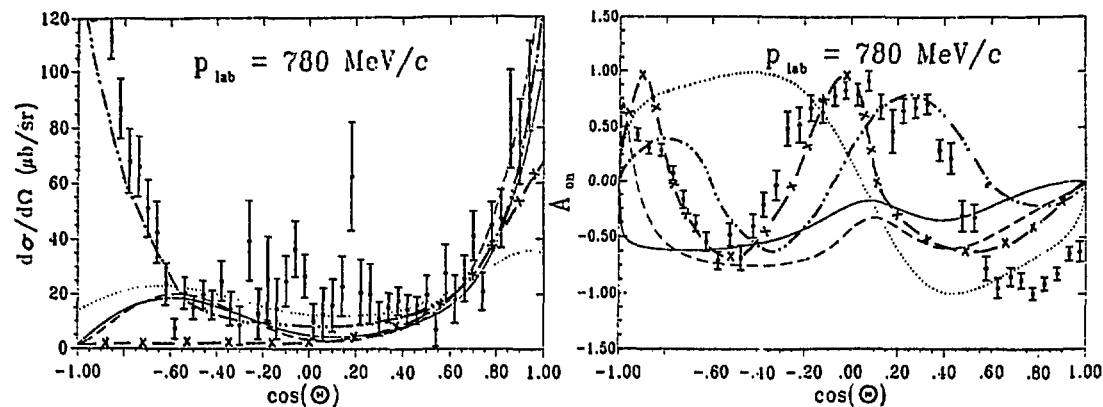


Figure 6. The $\bar{p}p \rightarrow \pi^+\pi^-$ annihilation : a) Differential cross section (data from ref. 27a)), b) analysing power (data from ref. 27b)). The models are from - ref. 21) : A(BOX) — , A(OBE) ----, C..... ; - ref. 26) : A(BOX) + $\pi^+\pi^-$ final state interaction : — x — x and from - ref. 20b) : — .. — ..

2.3 $\bar{N}N$ annihilation with statistical models

There is some evidence that many features of $\bar{p}p$ annihilation into mesons are statistical. Based on this a relatively simple phenomenological expression was proposed by Vandermeulen²⁹⁾ to reproduce the empirical branching ratios. He assumed that $\bar{N}N$ annihilation occurs exclusively via 2-meson production with nearest threshold dominance (see exponential factor in eq. 11). These 2 intermediate states of masses m_i and m_j subsequently decay into pions and kaons according to their empirical widths. He parametrised B_{ij} as

$$B_{ij}(E) = r_k (2J_i + 1)(2J_j + 1) W(I_i, I_j) 2^{-\delta_{ij}} p(E, m_i, m_j) e^{-A(E^2 - (m_i + m_j)^2)^{1/2}} \quad (11)$$

In this formula, r_k is 1 for non strange meson production and 0.15 for strange meson pair production (suppression), $(2J_i + 1)(2J_j + 1)$ is the spin weight, $W(I_i, I_j)$ the isospin weight (Clebsch-Gordan coefficients) and p the c.m. momentum describing the phase space factor. The parameter, $A = 1.2 \text{ GeV}^{-1}$, common to all channels is determined to fit the trend of the $\pi^+\pi^-$ cross section. The model reproduces well the pion multiplicity distribution such as $n\pi^+n\pi^-\pi^0$ over a wide range of energy up to $p_{\text{Lab}} < 3 \text{ GeV}/c$. A is related to the scale of the annihilation range given by the microscopic annihilation mechanism.

In averaging over spin and isospin as in eq. (11) important explicit angular momentum dependence is lost³⁰⁾. This lack of selection rule has been removed in ref. 25b) where, in the 2 meson doorway state, in analogy to the theory of compound nuclear reactions, one keep track of the relevant partial wave. This allows to introduce geometrical aspects and the annihilation dynamic is governed by the overlap of baryon density distributions of nucleon and antinucleon. The energy dependence of partial cross sections, in important channels, are well reproduced for a baryon, meson radii of .6 fm and pion

and kaon radii of .3 fm. A S-wave suppression is needed to describe the $\pi^+\pi^-$ and K^+K^- angular distribution.

3. THE $\bar{N}N$ ELASTIC AND CHARGE EXCHANGE SCATTERING

The use of Schrödinger equation (with relativistic kinematics) to solve the $\bar{N}N$ problem at low energy is as good as in the case of the low energy NN scattering. Here however one has to take into account of the annihilation processes and the use of coupled channel equations is the most appropriate tool. Let us restrict ourselves to 2 annihilation channels, e.g., channel a, with 2-meson M_1, M_2 production and channel b with 3-meson M_1, M_2, M_3 production. Following Green²⁸⁾ one can write, in a very schematic way, in the configuration space

$$[K(\bar{N}N) + V(\bar{N}N, \text{non annihilation}) - E]\psi_0(\bar{N}N) + \sum_{n=a,b} \langle \bar{N}N | V | n \rangle \psi(n) = 0 \quad (12)$$

and for each $n = a, b$

$$[K(n) - (E - m_1 - \dots)]\psi(n) + \langle n | V | \bar{N}N \rangle \psi_0(\bar{N}N) = 0 \quad (13)$$

If the mesons are not interacting one can report $\psi(n)$ from (13) into (12) and one obtains

$$[K(\bar{N}N) + V(\bar{N}N, \text{non annihilation}) - E]\psi_0(\bar{N}N) + W(\bar{N}N \rightarrow n \rightarrow \bar{N}N, \text{annihilation})\psi_0(\bar{N}N) = 0 \quad (14)$$

$$\text{with } W(\bar{N}N \rightarrow n \rightarrow \bar{N}N, \text{annihilation}) = - \sum_{n=a,b} \frac{\langle \bar{N}N | V | n \rangle \langle n | V | \bar{N}N \rangle}{[K(n) - (E - m_1 - \dots)]} \quad (15)$$

This equation defines the optical potential. The W annihilation will be complex with mesons thresholds. It is energy dependent and spin (tensor, spin orbit...) - isospin dependent. It will be in general non-local. W is generated by the iteration of the annihilation into mesons. It can be calculated from the annihilation amplitudes described in the previous section either from microscopic quark (2.1) - or meson (2.2) - degrees of freedom or more phenomenologically from the statistical approach (2.3).

Let us furthermore recall that in the $\bar{N}N$ channel space, starting from the $\bar{p}p$ initial state, from which most of the available experimental information comes, one has the elastic channel, $\bar{p}p \rightarrow \bar{p}p$ and the charge exchange (CEX) one, $\bar{p}p \rightarrow \bar{n}n$. Assuming isospin conservation one has

$$\begin{aligned} \langle \bar{p}p | T | \bar{p}p \rangle &= \langle \bar{n}n | T | \bar{n}n \rangle = (T_0 + T_1)/2 \\ \langle \bar{p}p | T | \bar{n}n \rangle &= \langle \bar{n}n | T | \bar{p}p \rangle = (-T_0 + T_1)/2 \end{aligned} \quad (16)$$

Here T_0 and T_1 are the isospin 0 or 1 amplitude respectively. Note also that $\langle \bar{p}n | T | \bar{p}n \rangle = \langle \bar{n}p | T | \bar{n}p \rangle = T_1$, however experimental results³¹⁾ on these reactions, more difficult to perform, are less numerous and less precise. In the $\bar{N}N$ channel one can work either in the isospin or particle basis.

3.1 Coupled channel approaches

As we have seen in section 2.2 the same authors as MH3 have built a microscopic model²⁴⁾ for the $\bar{N}N$ interaction based on meson-baryon dynamic (model C of table 1). They solve, in the isospin basis, the following coupled equations analogous to eqs. (14) and (15) but in momentum space

$$\begin{aligned} \langle \bar{N}N | T | \bar{N}N \rangle &= \langle \bar{N}N | V_{\text{eff}} | \bar{N}N \rangle + \langle \bar{N}N | V_{\text{eff}} | \bar{N}N \rangle G_0(\bar{N}N) \langle \bar{N}N | T | \bar{N}N \rangle \quad (17) \\ \text{with } \langle \bar{N}N | V_{\text{eff}} | \bar{N}N \rangle &= \langle \bar{N}N | V | \bar{N}N \rangle + \sum_B \langle \bar{N}N | V | \bar{B}B \rangle G_0(B) \langle \bar{B}B | V | \bar{N}N \rangle \\ &+ \sum_M \langle \bar{N}N | V | M_i M_j \rangle G_0(M) \langle M_i M_j | V | \bar{N}N \rangle \quad (18) \end{aligned}$$

Basically the first 2 terms of eq. 18 (baryon-exchanges, $B = N, \Delta$, in the s-channel, meson-exchanges in the t-channel) are taken from the G-parity transformation of the full Bonn NN potential²²⁾ (which includes $\pi, \rho, \omega, \sigma', \delta$ exchange plus baryon exchange N, Δ processes with two-meson intermediate states involving π and ρ) with some slight modification. The last term, the annihilation part, is the second iteration of the transition potential as described in section 2.2 (see also fig. 5). As expected and in contrast to semi-phenomenological models A (see table 1) the microscopic model C is energy and state dependent. Although various two-meson annihilation channels are treated explicitly (see section 2.2), these account for at most 30% of the total observed annihilation. Scaling to the empirical cross section was obtained in adjusting the form factors at the meson vertex of the transition potential. This difficulty of saturating totally the annihilation had already been pointed out in the hadronic approach of Moussallam^{20a)}, where the optical potential was calculated from a box diagram (see fig. 7) with 2-meson intermediate state, 2nd iteration of the diagram of fig. 3, this correspond to eq. 15 with $n = a$. Moussallam could not produce more than about 40% of the annihilation even with around 20 - meson channels.

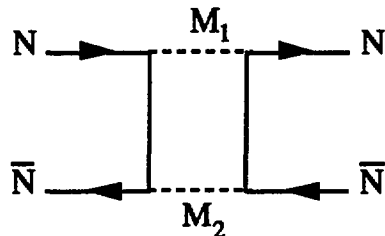


Figure 7. $\bar{N}N$ annihilation box diagram

Although the microscopic model C reproduces the total and elastic cross-section as well as the more phenomenologic models A, it fails in reproducing the elastic $d\sigma/d\Omega$ at $\theta_{cm} > 60^\circ$, the elastic polarization data and the CEX $d\sigma/d\Omega$ data. As concluded by the authors²⁴⁾

this failure of the microscopic spin-isospin dependence might be due to the fact that i) more transition channels (heavier 1^+ and 2^+ mesons) should be included ii) meson-meson interaction might be important (see sect. 2.2).

A recent phase shift analysis, constrained by the elastic long range one-pion exchange potential (OPEP), of pbar-p elastic and CEX data has been performed in ref. 32. The authors solve coupled channel equations in the particle basis (which allows to take into account more easily the mass differences) with a phenomenological complex energy dependent boundary condition for the short range. The best chi-square, in particular in CEX seems to favor a lower value $g_c^2 = 13.6 \pm .3$ of the charged π -N coupling constant than the commonly used 14.4 value^{32b)}. In the hadronic picture one should also be aware of i) the full coupled channel fit to the pbar-p, nbar-n, K - K^+ and π - π^+ data of ref. 33), ii) the comparison between coupled channel and optical models made by Shapiro and collaborators³⁴⁾ in studying the large P-wave contribution to the Nbar-N interaction at low energy.

3.2 Optical models

As we have seen in eqs. (14) and (15) the use of optical potential allows to treat in an average way the many mesonic annihilation channels. The early Nbar-N optical models^{35,36a)} the parameter of which were fitted to pre-LEAR data fails to reproduce the new data in particular the elastic³⁷⁾ and CEX³⁸⁾ analyzing power data. In view of this it might be interesting to reanalyse the theoretical models. Such a reanalysis, which we shall briefly describe here, has been recently done³⁹⁾ for the short range part of the Paris Nbar-N potential^{36a)}. The optical potential is written as

$$V_{NN}^- = U_{NN}^- - iW_{NN}^- \quad (19)$$

U_{NN}^- is the G-parity transform of the Paris NN potential^{36b)} for $r \geq 1$ fm with a phenomenological short range part arising from elastic annihilation processes. Let us recall that the Paris NN potential contains the OPEP, the two-pion-exchange (TPEP), the ω and A_1 meson exchange contributions. The TPEP was calculated via dispersion relations from the physical π N phase shifts and from the $\pi\pi$ - S and - P waves. The absorptive imaginary W has a form suggested by calculation^{20a)} of annihilation diagrams with 2-meson intermediate states (fig. 7). It is of short range, energy and state dependent :

$$W_{NN}^-(\vec{r}, T_L) = (g_c(1 + f_c T_L) + g_{ss}(1 + f_{ss} T_L) \vec{\sigma}_1 \cdot \vec{\sigma}_2 + g_T S_{12} + \frac{g_{LS}}{4m^2} \vec{L} \cdot \vec{S} \frac{1}{r} \frac{d}{dr}) \frac{K_0(2mr)}{r} \quad (20)$$

where m is the nucleon mass, T_L the pbar laboratory kinetic energy, $\vec{\sigma}_1 \cdot \vec{\sigma}_2$, S_{12} and $\vec{L} \cdot \vec{S}$ the usual spin-spin, tensor and spin-orbit invariants. The modified Bessel function $K_0(2mr)$ behaves as e^{-2mr} for large r .

The parameters of the core of this optical potential have been readjusted to obtain a best fit to about 2700 pbar-p data in the energy domain, $17 \text{ MeV} < T_L < 355 \text{ MeV}$ ($180 \text{ MeV}/c < p_L < 890 \text{ MeV}/c$). The old and new values for the parameters of W_{NN}^- shows some differences. One has, in particular an increase in the $T = 1$ channel of the tensor force and a suppression of the spin-orbit force. Some results are illustrated in figs. 8 to 11. The χ^2/data for 2714 data is 6.7. This relatively high value reflects not only some deficiency of the model but also some inconsistencies in the experimental data, in particular in the elastic $d\sigma/d\Omega$ (see fig. 8) and also some very small errors attached to some measurements.

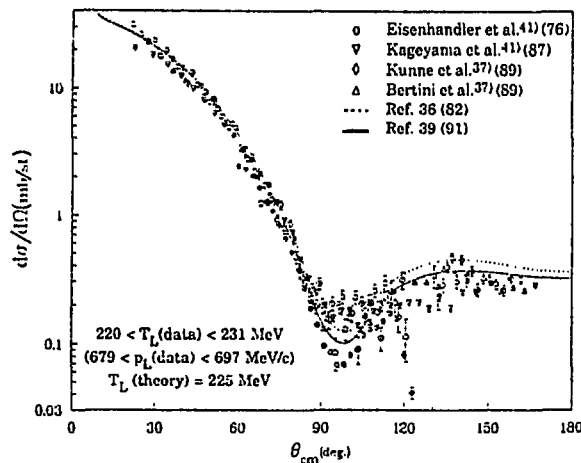


Figure 8. $\bar{p}p$ elastic $d\sigma/d\Omega$

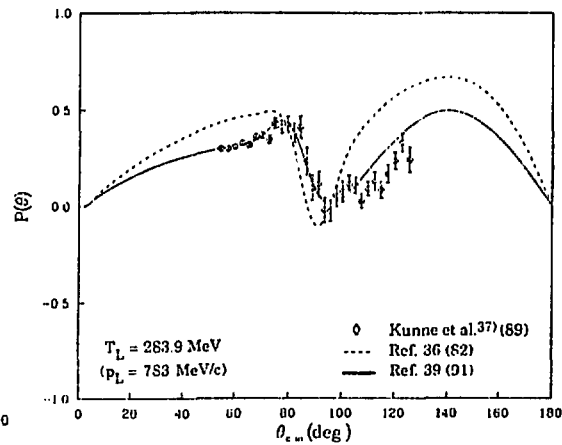
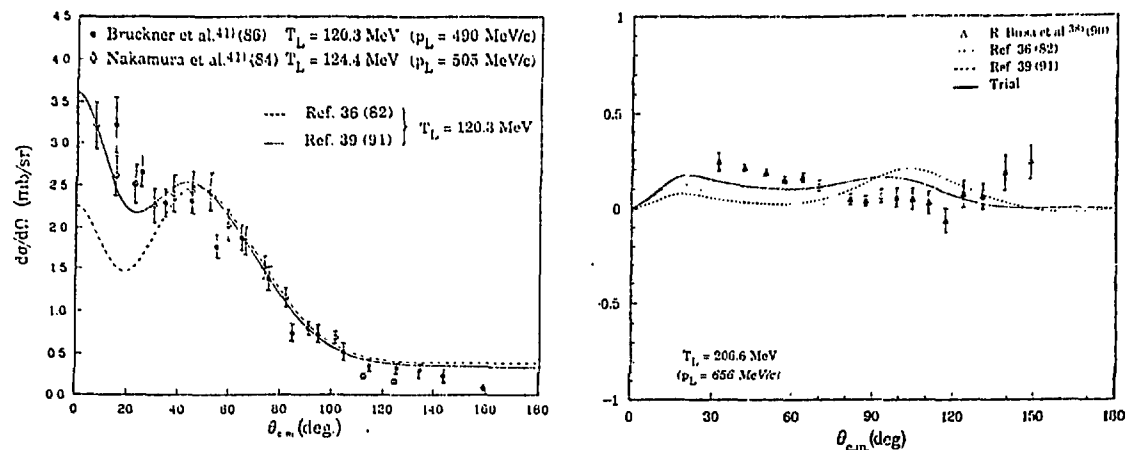


Figure 9. $\bar{p}p$ elastic polarization

The model does not predict well the recent CEX analysing power at 206.6 MeV³⁸ (fig. 11). This is an interesting fact as so far the spin dependent short range parameters (real and imaginary) were mainly constrained from pbar-p polarisation in their isospin (0+1) combination (see eq. 16). The CEX polarisation experiments constraining the isospin (0-1) combination allows to break the degeneracy. A trial solution, giving different isospin weights to the short range parameters of the spin forces is seen (solid line) to improve the prediction.

This analysis shows the interdependence between the pbar-p data and the short range Nbar-N interaction. The long and intermediate range force being theoretically constrained this newly determined short range could provide some hints for microscopic Nbar-N annihilation calculation.



4. OUTLOOK, DISCUSSION AND CONCLUSIONS

Let us first mention some further problems or related works. The potential models do not usually fit the behavior of the ρ ($\text{Re}F(o)/\text{Im}F(o)$) parameter close to threshold. See e.g. ref. 42) for a discussion on that matter. There now exists numerous spin-dependent data of very high quality from LEAR of the antihyperon-hyperon pair creation in $p\bar{p}$ scattering⁴³⁾. Although the threshold of these processes, $p_L = 1.435$ GeV/c, is at higher energy than those considered here, one can test also quark or/and meson degrees of freedom in these reactions⁴⁴⁾. The $N\bar{p}$ -Nucleus processes are also a tool to test our knowledge on the $N\bar{p}$ -N interaction, let us mention here the work of Locher and collaborators⁴⁵⁾ which studies in particular the properties of $p\bar{p}$ from $p\bar{p}$ -d annihilation at rest.

What have we learnt so far in the $N\bar{p}$ -N interaction? Let us summarize the situation. From the G-parity transform⁴⁶⁾ from NN to $N\bar{p}$ -N potential i) the OPEP changes its sign, the ρ does not, consequently their tensor force add and one then expects in $N\bar{p}$ -N strong tensor effect^{47a),34b)} ii) the ω changes its sign and becomes attractive and adds to the 2π -exchange attraction coming from 2π correlated in S-wave e.g. in NN Paris^{36b)}, or σ in OBE exchange as in Bonn²²⁾, Nijmegen^{35d)} and 2π exchange with $N\Delta$ intermediate states (Bonn²²⁾, Paris^{36b)}) and eventually to attractive $\pi\rho$ exchanges (full Bonn²²⁾). From i) and ii) one expects $N\bar{p}$ -N bound states or resonant states near threshold which are partly weakened by the very strong empirical annihilation^{34),48)}. This leads to the interpretation of the AX(1565) as a $^{13}P_2 - ^{13}F_2$ bound state of $N\bar{p}$ -N system^{47b)}. This intermediate range attraction ($1 < r < 1.5$ fm) is needed to reproduce the data: one cannot do without it and many phenomenological annihilation potential³⁵⁾ have even added a real attractive part in this range (see also annihilation part of models A(BOX) and A(OBE) in table 1). It is interesting to study to which component of the potential and/or to which meson exchange different observables are sensitive^{35c),47a),49)}. For instance the forward CEX $d\sigma/d\Omega$ is sensitive to OPEP which in this particular process is

enhanced by a isospin weight of 4 ($-\langle I=0|\tau'\cdot\tau^2|I=0\rangle + \langle I=1|\tau'\cdot\tau^2|I=1\rangle$). See also the study of helicity amplitude contributions to elastic pbar-p and CEX $d\sigma/d\Omega$ of ref. 50). So far no quark model has succeeded to generate the long and intermediate range mesons forces, the hadronic picture is certainly for the peripheral elastic Nbar-N interaction at his best.

What about the annihilation ? It was early realized that if one wants to reproduce the total cross section in the potential approach, the annihilation is strong and although being short ranged, $(2m)^{-1} \sim .1$ fm (from point like particle argument) most of the time its characteristic size is of the order of 100 MeV around 1 fm¹). This could be also seen as an indication of the structure of the nucleon as composit object. If one represents the annihilation by a short range exponential type function then it has to be scaled by a large number.

There has been a nice quantum mechanical formula to characterize the radius of annihilation and it was found to be of the order of 1 fm (state and energy dependent)⁵¹). It has been however found that the radius of annihilation of the Nbar-N Paris potential^{36a}) was smaller. As discussed in the introduction from the quark core picture surrounded by mesons one expects the annihilation to start when the core overlaps which justifies the geometrical picture and the chiral soliton type of approach of ref. 52). Here the quark degrees of freedom seems to be more appropriate and the QLD together with 3P_0 (eventually 3S_1) vertices has some success in particular in the planar annihilation in 2(A2) and 3(A3) mesons, however diagrams with quark rearrangement, R2, R3 and mixed are not rules out. It seems that, for microscopic calculation of annihilation, in particular into 3 mesons, quark models are at their best.

However so far calculations either from hadronic picture or quark model are parameter dependent. In the first approach the short range is unknown (form factors, e.g. Bonn potential or phenomenology, e.g. Nijmegen, Paris). This short range could be, in principle, calculated from QCD inspired models (non relativistic quark cluster type calculation with color screening to suppress Van der Vals forces but the annihilation mechanism does complicate the picture). In the second, the size of the 3P_0 (3S_1) coupling is empirical, although there is some estimate from lattice QCD in the strong coupling limit (flux tube model). One is naturally lead to think to a complementary picture : for the long range meson-hadron degree of freedom and for the short range quark degree of freedom (see e.g. ref. 50).

The combined study of the NN, Nbar-N interactions and Nbar-N annihilation into mesons should give us more knowledge on the internal structure of baryons and mesons and on their mutual interactions.

I would like to thank R. Vinh Mau, M. Lacombe and M. Pignone for fruitful discussions and B. Moussallam for useful comments.

5. REFERENCES

- 1 B.O. Kerbikov, L.A. Kondratyuk and M.G. Sapozhnikov, Sov. Phys. Usp. **32** (1989) 739, transl. Usp. Fiz. Nauk. **159** (1989) 3.
- 2 IX Europ. Symp. Nbar-N-Interactions and Fundamental Symmetries, Mainz 1988, K. Kleinknecht and E. Klempt (eds), Nucl. Phys. B (Proc. Suppl.) **8**, 1989)

- 3 Proceedings of the 1rst Biennial Conference on Low Energy Antiproton Physics, Stockholm, 1990, edited by P. Carlson, A. Kerek, S. Szilagyi (World Scientific, Singapore, 1991).
- 4 Workshop on Nucleon-Antinucleon Interactions, 8-11 July 1991, Moscow (Inst. of Physics, B. Chermushkinskaya 25 SU-11 7259 Moscow).
- 5 Nbar-N Interaction and Potential Models, October 6-8, 1991, Geneva, copies of contributions available from R. Hess, (University of Geneva, Physics Department 24, quai Ernest-Ansermet, CH-1211 Genève 4)
- 6 M. Maruyama, Theoretical aspects of Nbar-N annihilation in ref. 3, p.3.
- 7 H. Genz, M. Martinis, S.Tatur, Z. Phys. **A335** (1990) 87.
- 8 S. Okubo, Phys. Rev. **D16** (1977) 2336.
- 9 a) P. Blüm, G. Büche, H. Koch, Antiproton-proton annihilation at rest. Nov. 1988, Kernforschungszentrum Karlsruhe. b) C. Amsler, Nucl. Phys. **A508** (1990) 501c.
- 10 E. Klempt in ref. 3 p. 273 and in ref. 5, Systematics of Branching ratios.
- 11 J. Ellis, E. Gabathuler, M. Karliner, Phys. Lett. **B217** (1989) 173.
- 12 R. Kokoski, N. Isgur, Phys. Rev. **D35** (1987) 907.
- 13 N. Isgur, J. Paton, Phys. Rev. **D31** (1985) 2910.
- 14 S. Furui, Nucl. Phys. **A530** (1991) 717.
- 15 A.M. Green, G.Q. Liu, Nucl. Phys. **A486** (1988) 581.
- 16 M. Maruyama, S. Furui, A. Faessler, Nucl. Phys. **A472** (1987) 643.
- 17 T. Gutsche, M. Maruyama, A. Faessler, Nucl. Phys. **A503** (1989) 737.
- 18 S. Furui, G. Strobels, A. Faessler, R. Vinh Mau, Nucl. Phys. **A516** (1990) 643.
- 19 M. Maruyama, T. Gutsche, A. Faessler, G. Strobels, Phys. Rev. **C42** (1990) 716.
- 20 a) B. Moussallam, Nucl. Phys. **A407** (1983) 413; b) **A429** (1984) 429.
- 21 V. Mull, J. Haidenbauer, T. Hippchen, K. Holinde, Phys. Rev. **C44** (1991) 1337.
- 22 R. Machleidt, K. Holinde, CH. Elster, Phys. Rep. **149** (1987) 1.
- 23 B. Holzenkamp, K. Holinde, J. Speth, Nucl. Phys. **A500** (1989) 485.
- 24 T. Hippchen, J. Haidenbauer, K. Holinde and V. Mull, Phys. Rev. **C44** (1991) 1323.
- 25 a) S. Mundigl, M. Vicente Vacas, W. Weise, Z. Phys. **A338** (1991) 103; b) Nucl. Phys. **A523** (1991) 499.
- 26 V. Mull, K. Holinde, J. Speth, KFA-IKP(TH) 1991-37 Jülich preprint.
- 27 a) E. Eisenhandler et al., Nucl. Phys. **B96** (1975) 109.
b) R. Birsa et al., Nucl. Phys. (Proc. Suppl.) **B8** (1989) 141; F. Tassaroto et al. in ref. 3, p. 180.
- 28 A.M. Green in ref. 5, The Nbar-N interaction in terms of coupled channels.
- 29 J. Vandermeulen, Z. Phys. **37** (1988) 563.
- 30 C.B. Dover, Proc. Symp. on intersection between particle and nuclear physics, Rockport, Maine 1988, AIP proceedings. F. Myhrer in ref. 2 p. 193.
- 31 B. Gundersen et al., Phys. Rev. **D23** (1981) 587; T. Armstrong et al., Phys. Rev. **D36** (1987) 659.
- 32 a) R.G.E. Timmermans, Th. A. Rijken, J.J. de Swart, An antiproton-proton partial wave analysis, Nijmegen preprint (1991), see also contribution in ref. 5. b) Phys. Rev. Lett. **67** (1991) 1074.
- 33 G.Q. Liu, F. Tabakin, Phys. Rev. **C41** (1990) 665.
- 34 a) I.S. Shapiro, The main features of potential approach to Nbar-N interaction at low energies, contribution in ref. 5), b) J. Carbonell, O.D. Dalkarov, K.V. Protasov, I.S. Shapiro, CERN-TH 6096/91 preprint.

- 35 a) R.A. Bryan and R.J.N. Phillips, Nucl. Phys. **B5** (1968) 201. b) C. Dover, J-M. Richard, Phys. Rev. **C21** (1980) 1466; c) **C25** (1982) 1952. d) P.H. Timmers, W.A. van der Sanden, J.J. de Swart, Phys. Rev. **D29** (1984) 1928.
- 36 a) J. Côté, M. Lacombe, B. Loiseau, B. Moussallam, R. Vinh Mau, Phys. Rev. Lett. **48** (1982) 1319. b) M. Lacombe, B. Loiseau, J-M. Richard, R. Vinh Mau, J. Côté, P. Pirès, R. de Turreil, Phys. Rev. **C21** (1980) 861.
- 37 R. Bertini et al., Phys. Lett. **B228** (1989) 531. R.A. Kunne et al., Phys. Lett. **B206** (1988) 557; Nucl. Phys. **B323** (1989) 1.
- 38 R. Birsa et al., Phys. Lett. **B246** (1990) 267.
- 39 M. Pignone, M. Lacombe, B. Loiseau, R. Vinh Mau, Phys. Rev. Lett. **67** (1991) 2423. R. Vinh Mau, Analysis of the new pbar-p data with the Paris potential, in ref. 5).
- 40 R. Vinh Mau, in Proceedings of the 4th European Symposium on Nbar-N Interactions (CNRS, Paris 1979) p. 463.
- 41 E. Eisenhandler et al., Nucl. Phys. **B113** (1976) 1. T. Kageyama et al., Phys. Rev. **D35** (1987) 2655. W. Brückner et al., Phys. Lett. **169B** (1986) 302. K. Nakamura et al., Phys. Rev. **D29** (1984) 349.
- 42 F. Myhrer, Nucl. Phys. **A508** (1990) 513c. P. Kroll, W. Schweiger, Nucl. Phys. **A503** (1989) 865. B.V. Bykovskii, V.A. Meshcheryakov, D.V. Meshcheryakov, Yad. Fiz. **53** (1991) 257, transl. Sov. J. Nucl. Phys. **53** (1991) 1.
- 43 H. Schmitt, LEAR (PS 185), in ref. 5. T. Johanson et al., in ref. 3, p. 192.
- 44 W. Roberts, Z. Phys. **C49** (1991) 633. M.A. Alberg, E. M. Henley, W. Weise, Phys. Lett. **B255** (1991) 498. R.G.E. Timmermans, TH. A. Rijken, J.J. de Swart, Phys. Lett. **B257** (1991) 227. Strangeness exchange in antiproton-proton scattering, to be published in Phys. Rev. D. J. Haidenbauer et al., KFA-IKP(TH) 1991-31, Julich preprint and contribution to this conference. P. LaFrance, B. Loiseau, Nucl. Phys. **A528** (1991) 557. F. Tabakin, R.A. Eisenstein, Y. Lu, Phys. Rev. **C44** (1991) 1749.
- 45 M.P. Locher, B.S. Zou, Proton spectrum from pbar-d $\rightarrow 5\pi$ at rest PSI-PR-91-35 and contribution to this conference.
- 46 a) P. LaFrance, F. Lehar, B. Loiseau, P. Winternitz, Antinucleon-Nucleon scattering formalism and possible tests of CPT invariance, Saclay preprint, to be published in Helvetica Physica Acta. b) T.D. Lee, C.N. Yang, Nuovo Cimento **33** (1956) 749.
- 47 a) C.B. Dover, Precocious P-waves and coherent tensor forces, contribution in ref. 5. C.B. Dover, J-M. Richard, J. Carbonell, Phys. Rev. **C44** (1991) 1281. b) C.B. Dover, T. Gutsche, A. Faessler, Phys. Rev. **C43** (1991) 379. C.B. Dover, Quasinuclear Nbar-N states, contribution in ref. 5.
- 48 M. Lacombe, B. Loiseau, B. Moussallam, R. Vinh Mau, Phys. Rev. **C29** (1984) 1800.
- 49 F. Myhrer, Antinucleon Nucleon scattering, University of South Carolina preprint, 1991. B. Loiseau, J. de Phys. **C2-46** (1985) 339.
- 50 J. Haidenbauer, T. Hippchen, R. Tegen, Phys. Rev. **C44** (1991) 1812.
- 51 B. Povh, T. Walcher, Comments Nucl. Phys. **16** (1986) 85. T.A. Shibata, Phys. Lett. **189B** (1987) 232. J. Haidenbauer, T. Hippchen, K. Holinde J. Speth, Z. für Physik **A334** (1989) 467.
- 52 M.M. Musakhanov, I.V. Musato, Nucleon-Antinucleon Annihilation in chiral soliton model, Taskent state university preprint and contribution to this conference.